ASSESSMENT OF THE COLLAPSE RESISTANCE OF STEEL MRFs EQUIPPED WITH FLUID VISCOUS DAMPERS

Choung-Yeol Seo
Bechtel Power Corporation, Frederick, MD, USA

T.L. Karavasilis
School of Engineering, University of Warwick, Coventry, UK

James M., Ricles & Richard Sause
Department of Civil and Environmental Engineering, Lehigh University, Bethlehem, PA, USA

SUMMARY:
This paper evaluates the resistance against collapse of steel moment resisting frames (MRFs) with fluid viscous dampers. A simplified design procedure is used to design four different systems of steel MRFs with fluid viscous dampers where the strength of the steel MRF and the added damping ratio are varied. The combined systems are designed to achieve a performance that is similar or higher than that of conventional steel MRFs designed according to current seismic design codes. Based on the results of incremental nonlinear time history analyses, the probabilities of collapse of the frames with dampers are calculated and compared with those of conventional steel MRFs. The analytical frame models used in this study are reliably able to simulate global frame collapse by considering full geometric nonlinearities as well as the cyclic strength and stiffness deterioration of the structural steel members. The results of the study show that supplemental damping reduces the probability of collapse of a steel MRF with a given strength. However, it is also shown that supplemental damping does not guarantee a better collapse performance when the strength of the steel MRF with dampers is lower than 75% of the strength of a conventional MRF.

Keywords: Collapse fragility, Steel structure, Fluid viscous damper, Incremental dynamic analysis

1. INTRODUCTION

Passive damping systems can significantly improve the seismic performance of buildings by reducing drift and inelastic deformation demands on the primary lateral load resisting system, in addition to reducing the velocity and acceleration demands on non-structural components (Christopoulos and Filiatrault 2006). Among the different types of passive damping systems, viscous dampers have been extensively studied and used for the seismic design of new structures and the seismic upgrade of existing vulnerable structures (Symans et al. 2008). These dampers contain a closed cylinder filled with a fluid such as silicone oil, and a stainless steel piston with a piston rod and a piston head.

Individual fluid viscous damper tests have been performed and models to predict damper behavior under earthquake loading have been developed (Seleemah and Constantinou 1997). These studies have shown that the hysteresis of fluid viscous dampers can be accurately described by a nonlinear dashpot:

$$F_d = C \cdot |v|^a \cdot \text{sgn}(v) \qquad (1)$$

where F_d is the damper force output, C is the damping coefficient, α is the velocity exponent and *sgn* is the signum function. The exponent α typically ranges from 0.3 to 1.0.

The first design procedures for new buildings with passive dampers were published by the Structural Engineers Association of Northern California (Whittaker et al. 1993). These guidelines were developed on the basis that dampers will be located in a lateral force resisting system that already satisfies the strength and drift criteria of the current seismic code, with the goal of reducing earthquake

damage. The 2000 NEHRP provisions (BSSC 2001), however, allow a reduced design base shear force for the seismic design of buildings with passive damping systems where the expected performance is similar or higher than that of buildings with conventional lateral force resisting systems. Past research (e.g., Lee et al. 2009, and Karavasilis et al. 2012) confirmed that steel MRFs equipped with viscous type dampers can perform better under the design earthquake than a conventional steel MRF, even when the MRF with dampers is significantly lighter than the conventional MRF.

The recent ATC-63 document presents a new methodology for collapse assessment of structures under maximum considered earthquake (MCE) ground motions, with the aim to assess design criteria and seismic performance factors adopted in seismic codes (ATC 2009). A well designed structural system should provide a low probability of collapse (i.e., lower than 10%) under the MCE earthquake. In this methodology, the collapse margin ratio (CMR) is defined as the ratio of the ground motion intensity (i.e., spectral acceleration at the fundamental period of the structure) that causes one-half of the structures to form life-threatening collapse to MCE ground motion intensity. The acceptable value for the CMR varies depending on the seismic behavioral characteristics. The ATC-63 document highlights the need of applying the proposed collapse assessment methodology for structures equipped with damping systems in order to evaluate the damper design criteria of seismic provisions.

This paper evaluates the seismic resistance against collapse of steel MRFs with fluid viscous dampers. A simplified design procedure is used to design four different systems of steel MRFs with fluid viscous dampers in which the strength of the steel MRF and the added damping ratio are varied. The combined systems are designed to achieve a performance that is similar or higher than that of conventional steel MRFs designed according to current seismic codes. Based on the results of incremental dynamic analyses, probabilities of collapse of the frames with dampers are calculated and compared with those of conventional steel MRFs. The analytical results in the paper do not account for the effect of spectral shape at the fundamental period of the building, uncertainties in structural component properties, and the limit states of viscous dampers which can affect the collapse probabilities; these aspects and their effect on collapse are the subject of ongoing research by the authors.

2. PERFORMANCE BASED SEISMIC DESIGN OF STEEL MRFS WITH FLUID VISCOUS DAMPERS

2.1 Current Seismic Design Criteria
Current seismic provisions (e.g., BSSC 2001) specify that the design base shear force for the primary lateral force-resisting system of a building with dampers can be reduced to 75% of the design base shear of a conventional system without dampers. A steel MRF designed for a reduced base shear force would normally exceed the 2% drift limit of the seismic provisions. However, supplemental dampers are used to control drift demands on the flexible MRF and achieve a performance similar to that of a conventional frame (i.e., expected drift lower or equal to 2%) or higher performance (i.e., design drift significantly lower than 2%). This design philosophy offers significant benefits such as the reduction in steel weight of the MRF due to a reduced design base shear and higher performance due to the potential of passive dampers to reduce structural response.

2.2 Simplified Seismic Design Procedure for Buildings with Fluid Viscous Dampers
Lin and Chopra (2003) studied the peak displacement of an elastic SDOF system with a natural period T_n equipped with a viscous damper in series with a brace of stiffness K_b. The results of the study showed that the relation $\tau/T_n<0.02$ is satisfied for the practical range of values for the bracing stiffness K_b and the damping coefficient C, where τ is the relaxation time, i.e., $\tau =C/K_b$.

Ramirez et al. (2002) studied the relationship between the peak displacements of inelastic bilinear systems and corresponding linear elastic systems of the same period of vibration for high values of the viscous damping ratio. Their results showed that for systems with a period of vibration longer than 0.5 sec. that the equal-displacement rule is valid.

Christopoulos and Filiatrault (2006) proposed a distribution of damping coefficients proportional to the stiffness of the frame. In particular, the damping coefficient at each story is calculated equal to $C_i = \varepsilon K_{o,i}$, where $K_{o,i}$ is the horizontal story stiffness of the frame without dampers and ε is a constant. Given the damping coefficients C_i at each story i of the building and by assuming linear dampers ($\alpha=1$) positioned in a horizontal configuration, the equivalent damping ratio ξ_{eq} at the fundamental period of vibration T_1 under elastic conditions can be estimated according to the equation presented in Whittaker et al. (2003):

$$\xi_{eq} = \frac{T_1}{4\pi} \cdot \frac{\sum_i C_i (\varphi_i - \varphi_{i-1})^2}{\sum_i m_i \cdot \varphi_i^2} \qquad (2)$$

where φ_i and φ_{i-1} are the first modal displacements of stories i and i-1, respectively, and m_i is the mass of story i.

Based on the above discussion and given the properties of the MRF without dampers, a modified version of the simplified design procedure (SDP) developed by Lee et al. (2009) was adopted to design buildings with linear fluid viscous dampers and diagonal braces to achieve a target design drift. The modified SDP is given shown in Figure 1. A more detail description of the procedure can be found in Seo et al. (2012a)
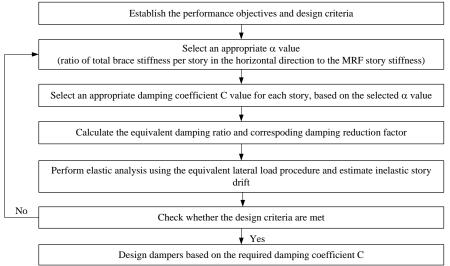

Figure 1. Modified simplified design procedure for MRF's with fluid viscous dampers

2.3 Prototype Building
Figure 2(a) shows the plan view of the 4-story, 7-bay by 7-bay prototype office building used for the study. The building is assumed to be located on a stiff soil site and has eight identical two-bay perimeter steel MRFs (two at each side) to resist lateral forces. The MRF is designed either as a conventional special moment resisting frame (SMRF), as defined in the 2003 International Building Code, IBC (ICC 2003), referred to herein as IBC 2003, or as an MRF equipped with linear fluid viscous dampers. In the latter case, dampers connected to the frame through chevron braces are added to the two bays of the MRF, as shown in Figure 2(b). The gravity (dead and live) loads considered in the design are those described in IBC 2003. A deterministic limit spectrum with parameters $S_S=1.5g$ and $S_1=0.6g$ represent the maximum considered earthquake (MCE), according to IBC2003. The design basis earthquake (DBE) has an intensity that is two-thirds that of the MCE.

The perimeter MRF of Figure 2(b) is designed as a conventional SMRF using the equivalent lateral force procedure from IBC 2003. This conventional SMRF without dampers, referred to herein as SMRF, satisfies the member strength criteria of the IBC 2003 with a response modification coefficient (i.e., strength reduction factor), R, equal to 8 and the 2% story drift limit of IBC 2003 with a deflection amplification factor, C_d, equal to 5.5. The design of the SMRF was controlled by drift.
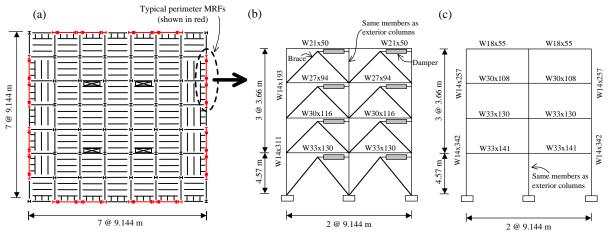
Figure 2. (a) Plan view of the prototype building, (b) Elevation of MRF with dampers and (c) Elevation of SMRF

Table 1. Summary of frame design

Design	Column sections	Beam sections	W_s (kN)	T_1 (sec)	C (kN·mm^{-1}·s.)*	ξ_{eq} (%)
SMRF	1st story : W14x342 2nd story: W14x342 3rd story: W14x257 4th story: W14x257	1st floor :W33x141 2nd floor:W33x130 3rd floor: W30x108 4th floor: W18x55	20205	1.70	N.A	N.A
CP100VLD	1st story : W14x311 2nd story: W14x311 3rd story: W14x193 4th story: W14x193	1st floor:W33x130 2nd floor: W30x116 3rd floor: W27x94 4th floor: W21x50	20205	1.87	1st story: 2.11 2nd story:1.70 3rd story: 1.06 4th story: 0.70	12.5
CP75VLD	Same as CP100VLD	Same as CP100VLD	26933	2.19	1st story: 3.24 2nd story: 2.64 3rd story: 1.79 4th story: 1.00	15.5
HP100VHD	Same as CP100VLD	Same as CP100VLD	20205	1.87	1st story: 4.22 2nd story:3.4 3rd story: 2.12 4th story: 1.4	23.8
HP75VHD	Same as CP100VLD	Same as CP100VLD	26933	2.19	1st story: 6.5 2nd story: 5.28 3rd story: 3.58 4th story: 2.00	32.5

For the MRFs with dampers, two different versions of the perimeter MRF were designed initially without dampers to have design base shears equal to 1.00V and 0.75V (where V is the design base shear of the SMRF) and without the 2% drift criteria. In particular, only the MRF with a design base shear equal to 1.00V was designed. The MRF with a design base shear equal to 0.75V was achieved by having the same cross sections with those of the MRF with a design base shear equal to 1.00V in conjunction with the seismic weight equal to (1/0.75) 1.333 times the seismic weight of the MRF with a design base shear equal to 1.00V. The two resulting MRF designs are lighter than the SMRF and do not comply with the 2% story drift design limit of IBC 2003. The supplemental linear fluid viscous dampers are then designed to control the story drift in these lighter MRFs using the simplified design procedure described above. The maximum story drift estimates for the damped MRFs are based on an equal displacement rule for checking compliance with the story drift design limit.

For each of the two lighter MRFs, two different damper designs were obtained with the aim to achieve a performance similar to that of the SMRF (i.e., designed for 2% story drift limit) or higher performance (i.e., designed for 1.5% story drift limit). The two resulting high-performance (highly damped) MRF designs with dampers are referred to herein as HP100VHD and HP75VHD while those with a conventional performance (lightly damped) are referred to herein as CP100VLD and

CP75VLD. The HP100VHD and CP100VLD MRFs with dampers result from the MRF with a design base shear equal to 1.00V, while the HD75VLD and CD75VLD MRFs with dampers result from the MRF with a design base shear 0.75V. The last two letters in the notation for the designs relate to the amount of damping added to the frame, where HD and LD stand for high and lightly damped, respectively.

Table 1 includes a summary of the properties of the SMRF and the four MRF designs with dampers (HP100VHD, HP75VHD, CP100VLD and CP75VLD). The table lists in sequence the column cross-sections, beam cross-sections, seismic weight (W_s), fundamental period of vibration of the structure without the dampers (T_1), damping constant (C) at each story, and equivalent viscous damping (ξ_{eq}). The damping constant (C) at each story is arrived at by satisfying the target story drift limit at each story level.

3. ANALYSIS AND DETERMINATION OF COLLAPSE STATE

3.1 Ground Motion Ensemble
A set of 22 recorded far-field ground motion pairs developed in the Applied Technology Council Project 63 (ATC 2009) is used in this study for nonlinear time history analysis. In this set, twenty-two record pairs were taken from 14 events which range in magnitude from 6.5 to 7.6, where the records were recorded on stiff soil (or soft rock) and do not exhibit pulse-type near-fault characteristics. It should be noted that the ground motion set used in this study does not represent extreme rare ground motions that have unique spectral shapes in the vicinity of the fundamental structural period (Baker and Cornell 2005) and, as a result, the performance assessment using the ground motion set can be conservative.

3.2 Analytical Frame Model
Ground motions along only one principle axis of the building's floor plan are considered. The analytical model in the study is a 2-D model of one-half of a perimeter frame of the 4-story building, considering two bays of the MRF and the associated tributary gravity load frames and seismic mass. The OpenSEES program (Mazzoni et al. 2006) is used to develop the analytical frame model in this study. The columns of the frame are modeled with a distributed plasticity force-based beam column element with five fiber sections along the element length. Each fiber is assigned a bilinear material model with a small positive post-yielding stiffness. The columns in the analytical model are assumed to exhibit stable cyclic behavior (i.e., no deterioration of strength or stiffness under cyclic loading), under large drift levels. This modeling assumption is reasonable since a typical seismically compact column section (e.g., W14 section) exhibits a large post-capping plastic rotation capacity for the full range of axial force expected in a column (Newell and Uang 2008).

The beams are modeled as elastic elements with a zero length plastic hinge rotational spring at their ends. The cyclic deterioration model developed by Lignos and Krawinkler (2007) was assigned to the zero length plastic hinge rotational springs. In this model, a backbone curve defines a reference skeleton for strength and deformation bounds of a structural component as well as a set of rules governing the hysteretic behavior between the bounds defined by the backbone curve. Cyclic deterioration characteristics in the model are defined by yield strength, post-capping strength, unloading stiffness, and reloading stiffness. The monotonic backbone curve for the moment–rotation relationship is illustrated in Figure 3 (a), where this curve is characterized by the elastic stiffness (K_e), a plastic rotation capacity and corresponding capped maximum strength ($\theta_{p.C}$ and M_c), a post-capping plastic rotation capacity and corresponding residual strength branch ($\theta_{pc.C}$ and M_r), as a fraction κ of the model yield strength (M_y), and a vertical branch indicating fracture. A typical hysteretic response showing cyclic strength and stiffness deterioration for the deterioration element is illustrated in Figure 3 (b).

To account for P-Δ effects, the gravity frame is modeled as a lean-on column with elastic beam-column elements incorporated with the co-rotational formulation available in OpenSEES. The floor mass is assigned to the lean-on column at each floor level in the model. A four sided planar element is used to capture important panel zone deformation modes including shear and symmetric column

bending deformations (Seo et al. 2012b). The damper and brace elements for the MRF with dampers are modeled with a linear elastic truss element. Linear viscosity is assigned as a material property for the damper element.
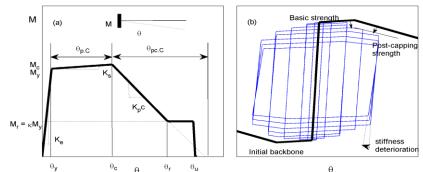

Figure 3. (a) Backbone curve, and (b) Cyclic moment rotation behaviour for the cyclic deterioration model

Rayleigh damping proportional to the mass and the tangent stiffness is assigned at the 1st and 3rd modal periods of the structure to account for structural inherent damping in the nonlinear time history analysis (NTHA). The same damping assumed in the design procedure is assigned at these periods.

It should be noted that the current analytical model can capture the cyclic deterioration of beam stiffness and strength, which can contribute to the global frame collapse. In the current analytical models, the diagonal braces are assumed to be strong enough not to buckle before the frame reaches its collapse capacity. In the analytical model, the damper limit states caused by their stroke limit are not considered, which may be an important consideration in the assessment of collapse fragility of frames equipped with fluid viscous dampers with limited stroke. Typical damper stroke limits in the dampers available in the market range from ±80 to ±130 mm, however, strokes can be extensible up to ±900 mm upon request (Taylor Device Inc.). With an extended stroke limit, the dampers in the prototype buildings would not reach their limit states before the frame reaches laterally instability. Therefore, the analytical model in this study is still valid to assess collapse fragility of the frames without considering damper limit states in the model.

3.3 Incremental Dynamic Analysis

Incremental dynamic analysis (IDA) (Vamvatsikos and Cornell 2002) is employed for assessing the collapse potential of the frames in this study. IDA is used to detect the collapse capacity of the frame associated with a particular ground motion. In this method nonlinear time history analyses are performed, where the ground motion intensity measured by 5% damped spectral acceleration at the fundamental period of the structure, Sa,is systematically scaled up in small increments until the frame model becomes globally unstable under the lateral seismic forces. The frame collapse capacity intensity to a particular ground motion, denoted as Sa_{COL}, is defined by the Sa value equal to the maximum Sa value for the frame to have been stable but less than the minimum Sa value for the frame to cause collapse. A limit of 15% transient story drift was used to define an upper bound value for Sa_{COL}. The results of the IDA using a large number of ground motion records are presented as a plot of Sa versus the frame response quantity of interest (e.g., peak story drift) and used for the probabilistic evaluation of the collapse capacity.

4. ASSESSMENT OF COLLAPSE FRAGILITY

4.1 Static Pushover Analysis

Static pushover analyses are initially performed to investigate the lateral load-roof drift relationship for the frames considered in this paper. These analyses are performed using a static lateral force distribution derived from the equivalent lateral force procedure described in the IBC 2003. Figure 4 (a) shows the relationship between the normalized base shear (V/W_s), and roof drift (θ_{roof}). It is shown that the SMRF exhibits the highest base shear strength and initial stiffness, since members in the SMRF are larger and heavier than the MRFs with dampers. With the aid of supplemental damping, these MRFs are designed to have a smaller V/W_s (i.e., the frames are weaker and more flexible). It is shown

that the MRFs with a smaller V/W_s exhibits a smaller roof drift associated with the complete loss of the static lateral load resistance.
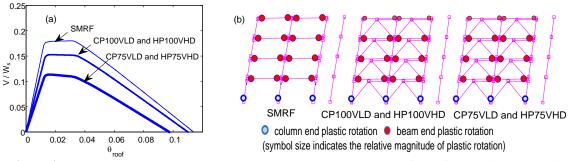

Figure 4. (a) Backbone curve, and (b) Cyclic moment rotation behaviour of the of the cyclic deterioration model

The post-yielding stiffness in the pushover curve becomes negative for the MRFs with dampers and its absolute value is larger for the MRFs with smaller V/W_s, indicating that the P-Δ effect is more pronounced for the weaker and more flexible MRFs with dampers. Figure 4 (b) illustrates the side sway mechanism of the frames considered in this study and relative magnitude of plastic hinge rotation at 9% roof drift predicted by pushover analysis, where plastic hinges form in the beam ends at all floor levels and in the column bases. As indicated in the figure, the frame design fulfills the strong-column-weak-beam (SCWB) philosophy under static lateral loads in accordance with AISC seismic specification (AISC 2005).
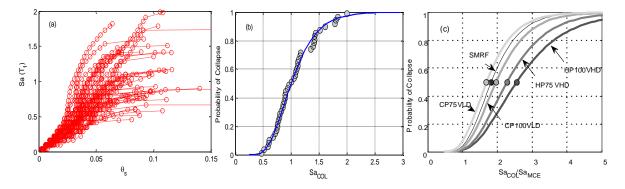
4.2 Collapse Fragility

Results of the IDA for the SMRF are plotted in Figure 5 (a), where a data point representing S_a and the corresponding maximum story drift θ_s is shown at each increment for each ground motion record. It is obvious that there is large variability in θ_s between records, even for the same frame at a specific ground motion intensity level. The slope of the IDA curve in general rapidly decreases and flattens out at some S_a level, meaning that at such intensity level, the story drift becomes very large with a small increase in ground motion intensity. For an individual record, the collapse capacity intensity (S_{aCOL}) of the frame model is defined as the S_a value at the end of the corresponding IDA curve. Figure 5 (a) illustrates that most of the IDA curves in general flatten out as θ_s exceeds 10% and, in many cases, the IDA curves terminate at a much lower story drift level.

S_{aCOL} from the IDA curves are ranked in ascending order. The collapse fragility curve is obtained by fitting a cumulative distribution function, assuming a lognormal distribution, to the ranked S_{aCOL} data points, as illustrated in Figure 5 (b) for the SMRF. It shows the cumulative distribution function fits well with the data points and validates the legitimacy of a lognormal distribution assumption. Although it is not shown in the paper, the lognormal distribution assumption still holds for S_{aCOL} of the MRFs with dampers considered in this study.

Fitted collapse fragility curves for all frames considered in this study are illustrated in Figure 5 (c), where Sa_{COL} is normalized by S_a at the MCE level, denoted as Sa_{MCE}. To quantify the structural safety margin against collapse in an earthquake, the collapse margin ratio (CMR) was calculated for each frame, where CMR is the ratio of the median Sa_{COL} ($\hat{S}a_{COL}$), to Sa_{MCE}. Assessment of the collapse potentials of all frames considered in this study is summarized in Table 2.

Figure 5 (c) shows that the collapse fragility curves for all frames studied, except for CP75VLD, are shifted to the right with respect to that for the SMRF (i.e., have a higher CMR than the SMRF). From this observation, it can be concluded that additional damping in general improves seismic resistance to frame collapse. In comparisons of the MRFs with dampers designed for the same target design performance level (i.e., CP100VLD versus CP75VLD or HP100VHD versus HP75VHD), the collapse fragility curves for the weak and more flexible MRFs (CP75VLD or HP75VHD) are shifted to the left with respect to the stronger and stiffer MRFs (CP100VLD or HP100VHD). This observation is confirmed by comparing the CMR values and the collapse probabilities at the MCE level for each

frame in Table 2. As noted above, the CMR for CP75VLD is lower than that of the SMRF; Table 2 indicates that the CMR for CP100VLD is higher than that of the SMRF, as is the CMR for HP75VHD where the maximum design drift is 1.5%. This result implies that the benefit of added damping on the frame collapse resistance cannot be fully utilized for relatively weak or flexible frames, and with frames whose design drift is too large. When a frame experiences significant lateral sway motion, the P-Δ effect can play an important role in cumulating drift. For a weak and flexible frame, this geometric nonlinearity effect is more pronounced in drifting the frame in one direction, where supplemental damping does not effectively help reduce the drift.
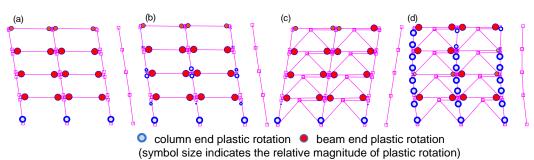

Figure 5. (a) Relationship between S_a and peak story drift θ_s resulting from IDA for SMRF, (b) Cumulative distribution of Sa_{COL} with a fitted curve for SMRF, and (c) Fitted cumulative distribution of S_{aCOL} for SMRF and MRFs with dampers considered in this study

Table 2. Summary of collapse analysis

Design	$\hat{S}a_{COL}$, g	$\delta_{Sa_{COL}}$ *	Sa_{MCE}, g	CMR	Prob. of collapse given Sa_{MCE}	$\hat{S}a_{COL}$, g
SMRF	1.00	1.42	0.55	1.83	4.4	1.00
CP100VLD	1.27	1.53	0.49	2.59	1.3	1.27
CP75VLD	0.97	1.47	0.43	2.26	1.7	0.97
HP100VHD	0.97	1.44	0.49	1.96	3.2	0.97
HP75VHD	0.72	1.41	0.43	1.69	7.8	0.72

* $\delta_{Sa_{COL}} = \exp(\sigma_{\ln Sa_{col}})$, where $\sigma_{\ln Sa_{col}}$ is the standard deviation of logarithm of Sa_{COL}

In order to examine how the SCWB philosophy avoids the concentration of damage in the column at a particular story at incipient collapse of a frame, the collapse mechanism and the location of the plastic hinges was examined. Figure 6 illustrates typical incipient collapse modes predicted by nonlinear time history analysis of each frame. The incipient collapse mode to a ground motion is captured at a slightly higher level than Sa_{COL}. Solid and hollow circles indicate beam and column plastic hinges, respectively. The relative magnitude of damage is indicated by the diameter of the circles. A typical collapse mode in the SMRF consists of a sway mechanism, characterized by large levels of plastic rotation at all floor beams and column bases as shown in Figure 6 (a). This collapse mode is well captured by static pushover analysis. In some cases, a mechanism characterized by plastic rotations at the column ends at some floor levels as shown in Figure 6 (b) with plastic hinges also forming in the beams. The formation of a distinct soft story mechanism, characterized by the formation of plastic hinges at the both ends of all columns at a particular story level, is not observed in the SMRF. A typical collapse mode observed in the MRFs with dampers is a sway mechanism, as shown in Figure 6 (c). In some cases, the collapse mode consists of a combination of beam and column plastic hinges. A collapse mode characterized by a distinctive soft-story mechanism is observed in the MRFs with dampers, as illustrated in Figure 6 (d). Out of 44 records, a soft-story mechanism occurs in HP100VHD for three ground motion records, in HP75VHD for two records, and in CP100VLD for one record. However, a soft-story mechanism does not occur in CP75VLD. The formation of a soft-story mechanism is partly attributed to high axial force demand on the columns of the MRFs with dampers. The axial force demand in columns is relatively high for a stiffer frame and the damping force transferred to the columns in an MRF with dampers tends to increase the axial force demand on the columns. Hence, the stiff and higher damped MRFs with dampers are more likely to develop a

soft-story mechanism. Since CP75VLD has the lowest CMR among all frames considered in this study, this observation may imply that frames with a soft-story collapse mechanism do not necessarily have a lower CMR than the frames with a sway mechanism with hinges in the beams and at the base of the ground floor columns.

○ column end plastic rotation   ● beam end plastic rotation
(symbol size indicates the relative magnitude of plastic rotation)

Figure 6. Typical incipient collapse modes (a) and (b) predicted for SMRF, and (c) and (d) predicted for MRFs with dampers.

5. SUMMARY AND CONCLUSIONS

In order to assess the collapse potential of steel moment resistant frames (MRFs) with and without fluid viscous dampers to selected ground motion intensity levels, analytical studies were performed using a set of ground motion records representative of a typical California earthquake. The MRFs with dampers considered in this study were designed with less steel weight and with the use of supplemental fluid viscous dampers to achieve a performance similar to, or higher than that of a conventional special steel moment resistant frame (SMRF). The analytical frame models are able to simulate global frame collapse reliably by considering geometric nonlinearities and using a phenomenological element that can capture cyclic deterioration in strength and stiffness of the structural components. Damper limit states were not, however, considered in the analytical models developed in this study.

Through a number of nonlinear time history analyses (NTHA), the collapse intensity level were obtained and examined to investigate the benefit of adding supplemental damping to the MRFs to enhance their seismic performance and increase their margin against collapse.

Record to record variability was considered in the estimate of the response by using multiple ground motion records. Uncertainty, however, due to unknown structural component properties and their variation were not considered in the analysis, which would otherwise increase the dispersion in the calculated response distribution. The ground motion records were used to represent a wide range of ground motion intensity levels by scaling them up or down. Consequently, the calculated response can substantially overestimate actual response, especially when it represents the response to a rare extreme earthquake. The conclusions drawn from the comparisons and the observations made in this study, however, still hold as follows:

- MRFs with supplemental damping can be designed with less weight to achieve similar or better performance than conventional SMRFs. This additional damping effectively decreases the probability of collapse.

- The reduction in strength can increase the probability of collapse (i.e., a frame with reduced strength would be less resilient to frame collapse) when the design drift it too large since the weak and more flexible frame is more vulnerable to P-Δ effects. Reducing the strength further below 75% of the minimum base shear capacity would not guarantee the levels of safety margin against collapse that are achieved by conventional SMRFs unless the drift is adequately controlled.

- An SMRF tends to form a sway mechanism with beam plastic hinges at incipient collapse and the strong-column-weak-beam philosophy in the design reduces the chance of having damage concentrated at a particular story (i.e., soft-story mechanism). Similarly, a typical incipient collapse mode in the MRFs with dampers is also a sway mechanism with beam plastic hinges. In

the MRFs with dampers a soft-story mechanism occurred and the likelihood of forming a soft-story mechanism increases for the stiffer or larger supplementally damped MRFs. The chance of having a soft-story mechanism at the incipient collapse is, however, still small for all frames considered in this study.

REFERENCES
AISC. (2005) *Seismic Provisions for Structural Steel Buildings*, American Institute of Steel Construction, Chicago, IL.
Applied Technology Council (2009). Quantification of building seismic performance factors, ATC-63 Project Report.
Baker JW, Cornell CA. (2005) A vector-valued ground motion intensity measure consisting of spectral acceleration and epsilon. *Earthquake Engineering and Structural Dynamics*, **34:10**, 1193-1217.
Building Seismic Safety Council (2001) NEHRP recommended provisions for seismic regulations for new buildings and other structures, Report FEMA 450, Federal Emergency Management Agency, Washington, D.C.
Christopoulos C, Filiatrault A. (2006) Principles of supplemental damping and seismic isolation. IUSS Press, Milan, Italy.
International Code Council (2003). International Building Code. Falls Church, VA
Karavasilis TL, Sause R, Ricles J. (2012) Seismic design of steel MRFs with compressed elastomer dampers. *Earthquake Engineering and Structural Dynamics*, **41:3**, 411-429.
Lee KS, Ricles J, Sause R. (2009) Performance based seismic design of steel MRFs with elastomeric dampers. (ASCE) *Journal of Structural Engineering*, **135:5**, 489-498.
Lignos DG, Krawinkler H. (2007) A database in support of modeling of component deterioration for collapse prediction of steel frame structures. *ASCE Structures Congress*, *SEI institute,* Long Beach CA.
Lin W-H, Chopra AK. (2003) Earthquake response of elastic single-degree-of-freedom systems with nonlinear viscoelastic dampers. (ASCE) *Journal of Engineering Mechanics* **129:6**, 597-606.
Mazzoni, S., McKenna, F., Scott, M. H., and Fenves, G. (2006) OpenSEES user's manual, 2006. Available from: www.opensees.berkeley.edu
Miyamoto HK, Gilani AS, Wada A, Ariyaratana C. (2010) Limit states and failure mechanisms of viscous dampers and the implications for large earthquakes. *Earthquake Engineering and Structural Dynamics*, in press.
Newell JD, Uang C-M. (2008) Cyclic behavior of steel wide-flange columns subjected to large drift. (ASCE) *Journal of Structural Engineering* **134:8**, 1334-1342.
Ramirez OM, Constantinou MC, Whittaker AS, Kircher CA, Chrysostomou CZ. (2002) Elastic and inelastic seismic response of buildings with damping systems. *Earthquake Spectra* **18:3**, 531-547.
Seleemah A, Constantinou MC. (1997) Investigation of seismic response of buildings with linear and nonlinear fluid viscous dampers. Report No. NCEER 97–0004, National Center for Earthquake Engineering Research, State Univ. of New York at Buffalo, Buffalo, N.Y.
Seo C-Y., Karavasilis TL, Ricles J, Sause R. Probabilistic assessment of the seismic collapse resistance of steel MRFs with viscous fluid dampers. In preparation for submission to *Earthquake Engineering and Structural Dynamics*
Seo C-Y., Ricles J, Sause R., Lin YC, Analytical models for 0.6 scale self-centering MRF with beam web friction devices. In preparation for submission to *Earthquake Engineering and Structural Dynamics*
Symans MD, Charney FA, Whittaker AS, Constantinou MC, Kircher CA, Johnson MW, McNamara RJ. (2008) Energy dissipation systems for seismic applications: current practice and recent developments. (ASCE) *Journal of Structural Engineering*, **134**:**1**, 3-21.
Taylor Devices inc. North Tonawanda, NY. Accessible to http://www.taylordevices.com
Whittaker AS, Aiken ID, Bergman D, Clark PW, Cohen JM, Kelly JM, Scholl RE. (1993) Code requirements for the design and implementation of passive energy dissipation systems, Proceedings, Seminar on Seismic Isolation, Passive Energy Dissipation, and Active Control, Report No. ATC-17-1, Applied Technology Council, Redwood City, CA.
Whittaker AS, Constantinou MC, Oscar MR, Johnson MW, Chrysostomou CZ. (2003) Equivalent lateral force and modal analysis procedures of the *2000 NEHRP Provisions* for buildings with damping systems. *Earthquake Spectra* **19:4,** 959-980.
Vamvatsikos D, Cornell C. A. (2002) Incremental dynamic analysis. *Earthquake Engineering and Structural Dynamics*, **31:3**, 491-514.